

Non-Uniform sampling in near field measurement: Experimental results

Maria Antonia Maisto⁽¹⁾, Raffaele Solimene⁽¹⁾, Giovanni Leone⁽¹⁾ and Rocco Pierri⁽¹⁾
 (1) Dipartimento di Ingegneria, Università degli Studi della Campania, 81031 Aversa, Italy

Abstract

In this paper, the problem of sampling the field radiated by a planar source observed over a finite planar aperture located in the near-field is addressed. In particular, the paper is devoted to assess the performance of the sampling strategy proposed in [9] in a real environment. Accordingly, such a strategy is compared to the classical half-wavelength sampling approach by processing some experimental data. It is shown that in spite of the resulting sampling points are much lower than the ones required by the half-wavelength sampling, the proposed strategy allows to obtain good results.

1 Introduction

Near field measurement techniques are the most advanced antenna testing procedures, currently used in most technologically advanced contexts. They consist of measuring the field radiated by the antenna under test at a short-range within an anechoic environment, by means of a probe whose position is mechanically scanned over planar, cylindrical, or spherical surfaces. Then, the measured data are numerically processed by the so-called "near/far-field transformations" to obtain the radiation pattern. Within this framework, the reduction of measurement point number is a very important issue since it impacts on acquisition time [1]-[4].

From a general perspective, such a task can be cast as a sensor selection problem [5], where one selects a finite number of positions among the ones available over a generally very dense grid. A number of methods, based on convex optimization, greedy procedure and heuristics, have been developed. By these ones, the selection is basically achieved by optimizing some metrics which are related to the singular values of the radiation operator [6, 7, 8].

In [9], a different approach that is not based on the iterative procedure is proposed. More in detail, said \mathcal{A} radiation operator, the problem is cast as the discretization of the composed operator $\mathcal{A}\mathcal{A}^\dagger$ (with \mathcal{A}^\dagger being the adjoint of the radiation operator) and the sampling points are chosen as the ones that allow approximating the more significant eigenvalues of $\mathcal{A}\mathcal{A}^\dagger$. To this end, thanks to a suitable variable transformation that 'warps' the spatial observation variables [10]-[11], the kernel function of $\mathcal{A}\mathcal{A}^\dagger$ is

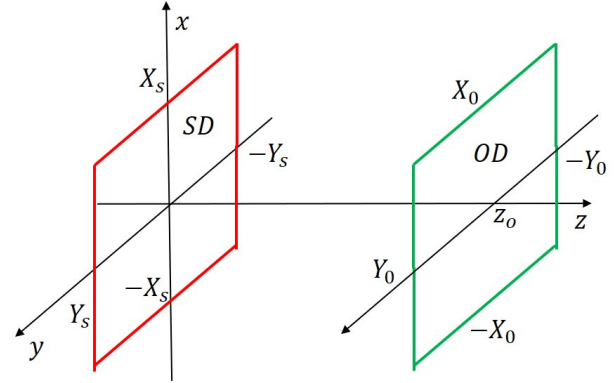


Figure 1. Geometry of the problem.

approximated as a band-limited function and then the Shannon sampling theorem is used for the discretization. In this paper, the performances of the sampling strategy proposed in [9] are assessed by processing experimental data. It is shown that in spite of the resulting sampling points are much lower than the ones required by the common half-wavelength sampling, the proposed strategy allows to obtain good results.

2 Experimental setup

In this section, we provide some experimental examples in order to assess the performance of the sampling strategy proposed in [9]. A pictorial view of experimental setup is reported in 1. Let λ be the wavelength. A radar array antenna whose equivalent magnetic current has a bounded finite planar support $SD = [-X_s, X_s] \times [-Y_s, Y_s]$ with $X_s = Y_s = 13.78\lambda$ is considered. Suppose to collect the field radiated data over another planar domain $OD = [-X_0, X_0] \times [-Y_0, Y_0]$ (i.e., the observation domain) with $X_0 = Y_0 = 25.1\lambda$ located in near-field at a distance $z_0 = 8.2\lambda$.

In [9], it is shown that by introducing the following warping variable [11] transformations

$$\begin{aligned} \xi_x : x_o &\rightarrow \\ \rightarrow \xi_x(x_o) &= \alpha_x \frac{k}{2} \left[\sqrt{(x_o + X_s)^2 + z_0^2} - \sqrt{(x_o - X_s)^2 + z_0^2} \right] \\ \xi_y : y_o &\rightarrow \end{aligned}$$

$$\rightarrow \xi_y(y_o) = \alpha_y \frac{k}{2} [\sqrt{(y_o + Y_s)^2 + z_o^2} - \sqrt{(y_o - Y_s)^2 + z_o^2}], \quad (1)$$

and

$$\begin{aligned} \gamma_x : x_o &\rightarrow \\ \rightarrow \gamma_x(x_o) &= \frac{k}{2} [\sqrt{(x_o + X_s)^2 + z_o^2} + \sqrt{(x_o - X_s)^2 + z_o^2}] \\ \gamma_y : y_o &\rightarrow \\ \rightarrow \gamma_y(y_o) &= \frac{k}{2} [\sqrt{(y_o + Y_s)^2 + z_o^2} + \sqrt{(y_o - Y_s)^2 + z_o^2}]. \quad (2) \end{aligned}$$

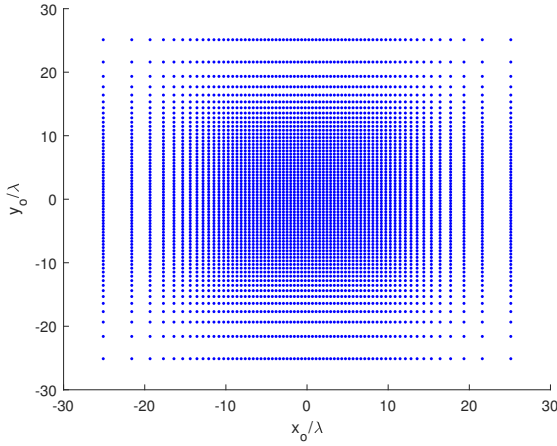


Figure 2. Illustrating the sampling points positions returned by proposed approach for $X_s = Y_s = 13.78\lambda$, $z_o = 8.2\lambda$, $X_o = Y_o = 25.1\lambda$ and $\alpha_x = \alpha_y = 1.3$

the field radiated by an antenna supported on SD , E , can be expanded as

$$\begin{aligned} E(\xi_x, \xi_y) &= e^{j\gamma_x(\xi_x)} e^{j\gamma_y(\xi_y)} \sum_{m,l} E(\xi_{xm}, \xi_{yl}) \\ &e^{-j\gamma_x(\xi_{xm})} e^{-j\gamma_y(\xi_{yl})} \text{sinc}[\xi_x - \xi_{xm}] \text{sinc}[\xi_y - \xi_{yl}], \quad (3) \end{aligned}$$

with $\xi_{xm} = m\pi$ and $\xi_{yl} = l\pi$ being the sampling points and m and l integer indexes. Note that the oversampling factors α_x and α_y allow controlling the representation error when OD is larger than SD . In [9], such factors are set to 1.3. In order to pass from the sampling points in (ξ_x, ξ_y) to the ones in (x_o, y_o) (the actual observation variables), Equation (1) must be used. For example, the sampling position along x_o , i.e., x_{om} , are obtained by solving for x_{om} the following equation

$$\xi_x(x_{om}) = m\pi \quad (4)$$

A similar equation of course holds true for the sampling points y_{ol} along the variable y_o . Since the non-linear linking between the warping variables ξ_x , ξ_y and x_o, y_o , this

sampling strategy leads to a non-uniform arrangement of observation points. In Fig. 2, the sampling point distribution returned by the proposed strategy for the considered experimental example is shown. It can be appreciated that the sampling step increases as the observation point approaches the edge of the measurement domain. It must be highlighted that the number of samples required by the non-uniform sampling scheme is actually much lower than the ones arising from a $\lambda/2$ sampling. Indeed, the proposed method requires $N = 4624$, whereas the $\lambda/2$ sampling requires 10404 samples.

The radiation pattern is evaluated by Fourier transforming (by means of a FFT procedure) the near-field data. In particular, as far as the non-uniform arrangement is under concern, the field is first interpolated over a uniform $\lambda/2$ grid and finally, Fourier transformed. In order to appreciate the capability of the proposed sampling method of approximating the radiated field, we use the following representation error metric (RE) computed over the measurement aperture, that is

$$RE_{dB}(X_o, Y_o) = 20 \log_{10} \frac{\|E - E_{\lambda/2}\|}{\|E_{\lambda/2}\|}, \quad (5)$$

where E is the near-field data collected on the non-uniform sampling scheme and then interpolated over a $\lambda/2$ grid, $E_{\lambda/2}$ is the near-field data directly collected over the uniform $\lambda/2$ grid and $\|\cdot\|$ is the Euclidean norm.

The Figures 3 and 4 show the radiation pattern results concerning the two different radiation patterns radiating by the considered radar: the sum and difference one.

In all figures, the radiation patterns are reported as a function of the normalized spectral variables $k_x/k = \sin \theta \cos \phi$ and $k_y/k = \sin \theta \sin \phi$, with θ and ϕ being the usual polar angles, and shown only for the so-called 'visible' domain, that is for $k_x^2 + k_y^2 = k^2$. Moreover, in all the figures is reported also $RE_{dB}(X_o, Y_o)$.

As concern the sum pattern, the results are reported in Fig. 3. As can be seen, in this case, the radiation pattern looks like a unique focusing beam with a side lobe level lower than $-40dB$. In spite of a very low side lobe, the representation error is about $-25dB$. In Fig. 4, the case of difference pattern is under concern. Same results as before in terms of representation error can be obtained. Accordingly, also in the real environment, the proposed sampling strategy allows obtaining results comparable to the ones returned by the more standard uniform $\lambda/2$ sampling, although the number of required points is reduced.

3 Conclusion

In this paper, the performances of the sampling strategy proposed in [9] are assessed by processing some experi-

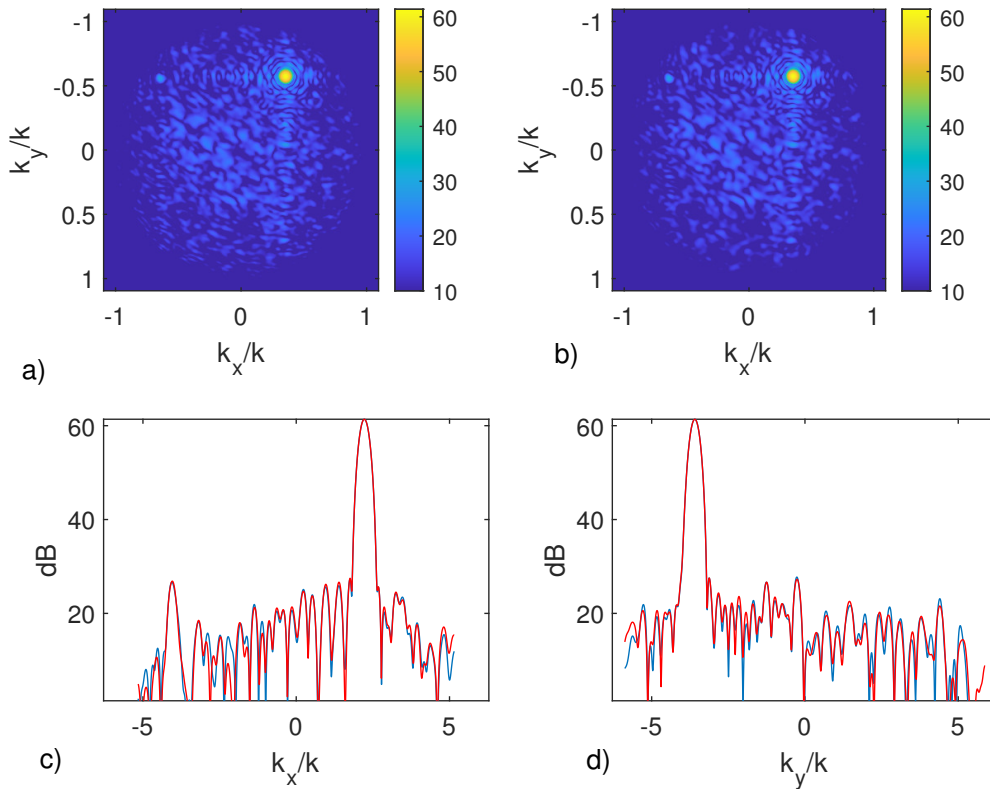


Figure 3. Amplitude of the sum radiation pattern for the steered direction $(\phi_s, \theta_s) = (-58.3^\circ, 42.2^\circ)$. In (1), the radiation pattern is obtained by employing the near-field data according to the proposed non-uniform sampling scheme and then interpolated over a $\lambda/2$ grid. In (2), the radiation pattern is obtained by directly employing the near-field data over a uniform $\lambda/2$ grid. Panels (3) and (4) show the radiation pattern cut-views passing through the main-beam maximum along k_x and k_y , respectively. The blue lines report the radiation pattern computed by using the uniform $\lambda/2$ sampling and the red ones show the radiation pattern obtained by the proposed method. The representation error is $RE_{dB}(25.1\lambda, 25.1\lambda) = -25dB$.

mental data. It is shown that in spite of the resulting sampling points are much lower than the ones required by the common half-wavelength sampling, the proposed strategy allows to obtain good results. Only a degradation of the side lobe level beyond the valid angle region is observed. Further theoretical investigations are required to compensate for such an effect.

4 Acknowledgements

This research was partially funded by the Italian Ministry of University and Research through the PON initiative under the project Leonardo 4.0 CUP B26C18000080005 and partially by the Università della Campania Luigi Vanvitelli, through Programma V:ALERE 2020, under the project Efficient Probe pOsitioning for Near-field Measurement techniques (EPONIMI) CUP: B66J20000680005. .

References

[1] O. M. Bucci, C. Gennarelli, and C. Savarese, "Representation of Electromagnetic Fields over Arbitrary Sur-

faces by a Finite and Nonredundant Number of Samples," *IEEE Trans. Antennas Propagat.*, **46**, 1998, pp. 351-359.

[2] M. A. Maisto, R. Solimene and R. Pierri, "Minimum Measurement Points in Near Field: Numerical Results," *Progress in Electromagnetics Research Symposium*, Toyama, Japan, 2018, pp. 2358-2361.

[3] M. A. Maisto, R. Solimene and R. Pierri, "Optimal choice of measurement points in near field: numerical results," *IEEE International Symposium on Antennas and Propagation USNC/URSI National Radio Science Meeting*, Boston, MA, USA, 2018, pp. 2561-2562.

[4] M. A. Maisto, R. Solimene and R. Pierri "Efficient Sampling of the Near Field Radiated by a Planar Source: Numerical Results" *Progress in Electromagnetics Research Symposium*, 17-20 June 2019, Rome, Italy.

[5] S. J. Reeves, and L. P. Heck "Selection of observations in signal reconstruction," *IEEE Trans. Signal Process.*, **43**, 1995, pp. 788-791.

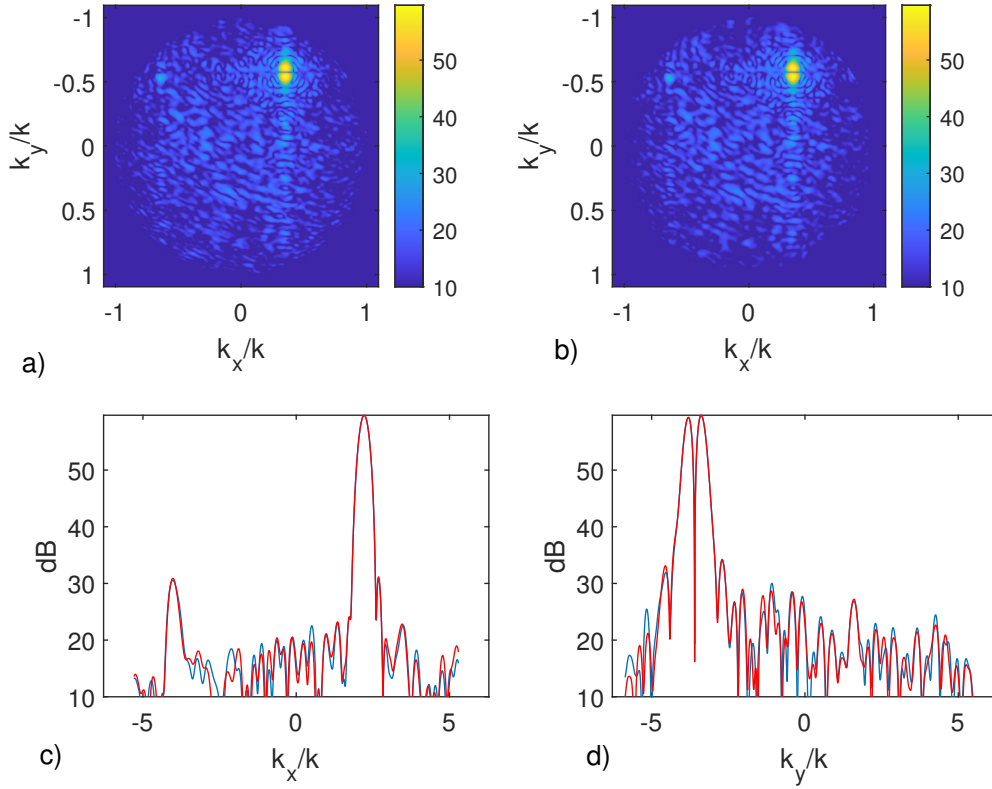


Figure 4. Amplitude of the difference radiation pattern for the steered direction $(\phi_s, \theta_s) = (-58.3^\circ, 42.2^\circ)$. In (1), the radiation pattern is obtained by employing the near-field data according to the proposed non-uniform sampling scheme and then interpolated over a $\lambda/2$ grid. In (2), the radiation pattern is obtained by directly employing the near-field data over a uniform $\lambda/2$ grid. Panels (3) and (4) show the radiation pattern cut-views passing through the main-beam maximum along k_x and k_y , respectively. The blue lines report the radiation pattern computed by using the uniform $\lambda/2$ sampling and the red ones show the radiation pattern obtained by the proposed method. The representation error is $RE_{dB}(25.1\lambda, 25.1\lambda) = -22dB$.

- [6] S. Joshi, and S. Boyd, "Sensor selection via convex optimization," *IEEE Trans. Signal Process.*, **57**, 2008, pp. 451-462.
- [7] J. Ranieri, A. Chebira, and M. Vetterli, "Near-optimal sensor placement for linear inverse problems", *IEEE Trans. Signal Process.*, **62**, 2014 pp. 1135-1146.
- [8] C. Jiang, Y. Soh, H. Li, "Sensor placement by maximal projection on minimum eigenspace for linear inverse problems," *IEEE Trans. Signal Process.*, **64**, 2016, pp. 5595-5610.
- [9] M. A. Maisto, R. Pierri, and R. Solimene, "Near-Field Warping Sampling Scheme for Broad-Side Antenna Characterization," *Electronics*, **9**, 2020, pp. 1047.
- [10] M. A. Maisto, R. Solimene, and R. Pierri, "Sampling approach for singular system computation of a radiation operator," *J. Opt. Soc. Am. A*, **36**, 2019, pp. 353-361.
- [11] M. A. Maisto, R. Solimene and R. Pierri, "Warping method for probe location in near/far field Transformation", *14th European Conference on Antennas and*

Propagation, in Copenhagen, Denmark, March 15-20, 2020.